Bull Volcanol (2003) 65:517–529
DOI 10.1007/s00445-003-0280-3

RESEARCH ARTICLE

V. Acocella · M. Neri

What makes flank eruptions? The 2001 Etna eruption and its possible triggering mechanisms

Received: 10 June 2002 / Accepted: 27 January 2003 / Published online: 6 March 2003

Abstract Most flank eruptions within a central stratovolcano are triggered by lateral draining of magma from its central conduit, and only few eruptions appear to be independent of the central conduit. In order to better highlight the dynamics of flank eruptions in a central stratovolcano, we review the eruptive history of Etna over the last 100 years. In particular, we take into consideration the Mount Etna eruption in 2001, which showed both summit activity and a flank eruption interpreted to be independent from the summit system. The eruption started with the emplacement of a ~N-S trending peripheral dike, responsible for the extrusion of 75% of the total volume of the erupted products. The rest of the magma was extruded through the summit conduit system (SE crater), feeding two radial dikes. The distribution of the seismicity and structures related to the propagation of the peripheral dike and volumetric considerations on the erupted magmas exclude a shallow connection between the summit and the peripheral magmatic systems during the eruption. Even though the summit and the peripheral magmatic systems were independent at shallow depths (<3 km b.s.l.), petro-chemical data suggest that a common magma rising from depth fed the two systems. This deep connection resulted in the extrusion of residual magma from the summit system and of new magma from the peripheral system. Gravitational stresses predominate at the surface, controlling the emplacement of the dikes radiating from the summit; conversely, regional tectonics, possibly related to N-S trending structures, remains the most likely factor to have controlled at depth the rise of magma feeding the peripheral eruption.

Keywords Central volcanoes · Summit and flank eruptions · Dikes · Tectonics · Volcano load · Mount Etna

Editorial responsibility: R. Cioni

V. Acocella (✉)
Dip. Scienze Geologiche Roma TRE,
Largo S.L. Murialdo 1, 00146 Roma, Italy
e-mail: acocella@uniroma3.it
Tel.: +39-06-54888043
Fax: +39-06-54888201

M. Neri
Istituto Nazionale di Geofisica e Vulcanologia,
Piazza Roma 2, 95123 Catania, Italy

Introduction

Central stratovolcanoes are characterized by summit and flank eruptions. Summit eruptions are the consequence of the extrusion of magma from a central reservoir through the summit conduit. Flank eruptions are commonly characterized by multiple aligned vents that radiate from the summit of the volcano (Fig. 1).

The long-term (10^2–10^3 years) relationships between summit and flank eruptions have been previously investigated, defining distinct patterns (Takada 1997). In the shorter term, within the time span of a single eruption, several aspects have also been highlighted. Most of the observed flank eruptions on stratovolcanoes with pro-

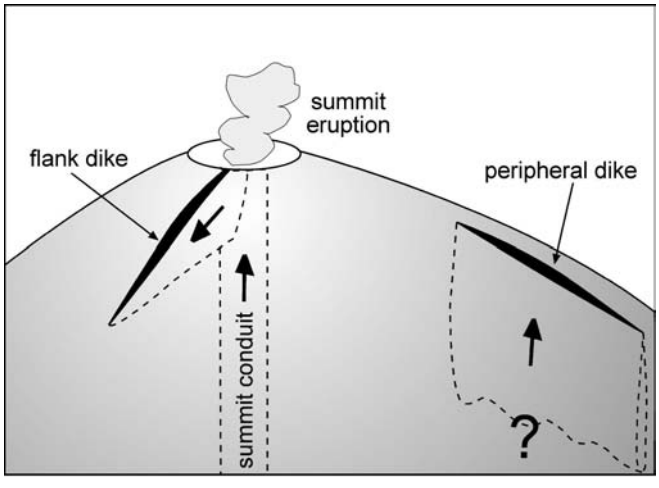

Fig. 1 Sketch showing the relationships between flank and summit eruptions developed within a central volcano

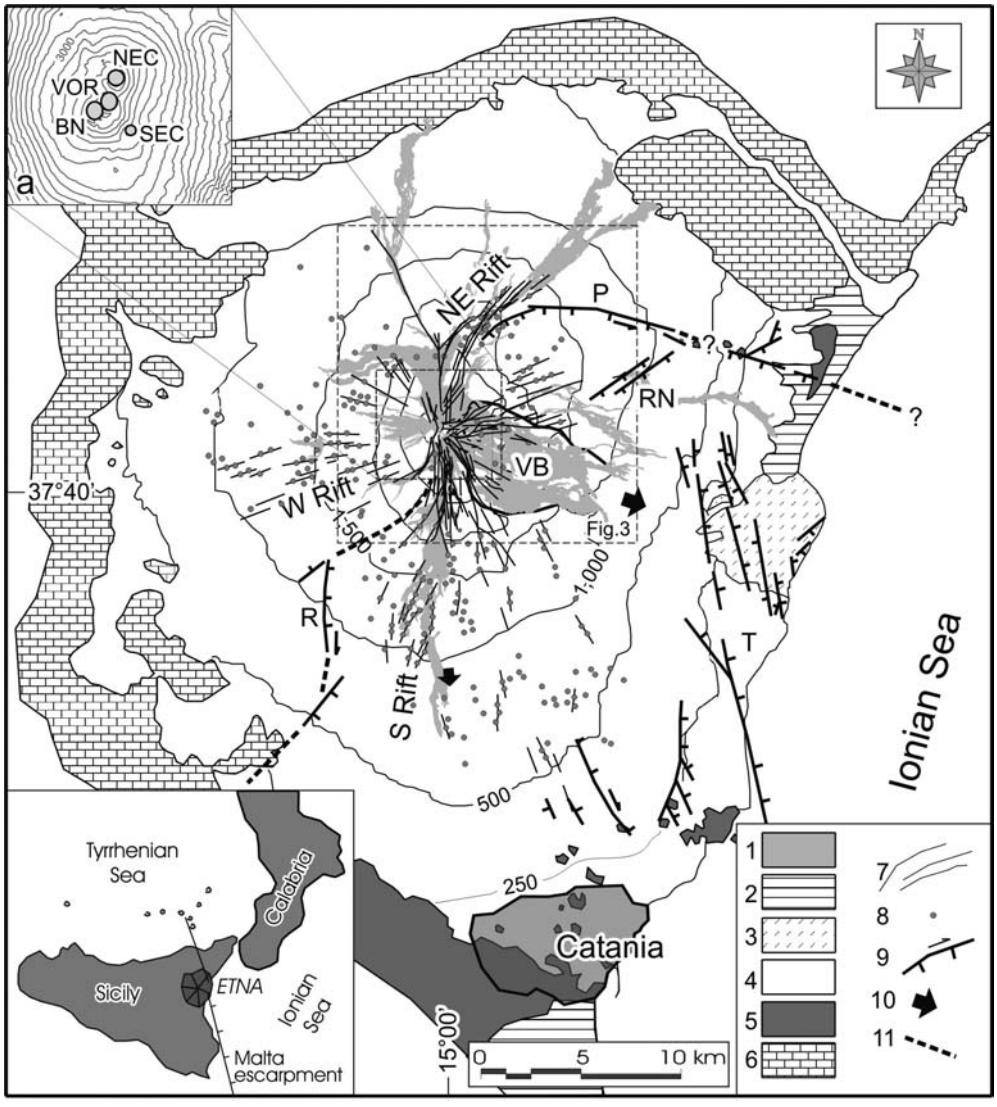

Fig. 2 Simplified geological and tectonic map of Mount Etna. The boundaries of the unstable sector of the volcano are taken from Borgia et al. (1992) and Rust and Neri (1996). The sedimentary basement is made up of units of the Apennine-Maghrebian Chain (N and W sectors) and of Early-Quaternary clays (S sector). *VB* Valle del Bove, *P* Pernicana Fault, *RN* Ripe della Naca Faults, *T* Acireale Faults, *R* Ragalna Faults. *1* 1900–2002 lava flows; *2* recent alluvium; *3* "Chiancone" deposit, originated from the emptying of Valle del Bove; *4* Etnean volcanics; *5* Early Quaternary clays; *6* Pre-Quaternary sedimentary rocks; *7* main eruptive fracture zones; *8* cinder cones; *9* main faults (*arrows* indicate lateral component of movement); *10* direction of displacement of the unstable sector; *11* boundaries of the unstable sector, question marks indicate uncertainty of some segments of the boundaries. Inset (**a**): Etnean summit craters. *VOR* Voragine; *NEC* North-East Crater; *BN* Bocca Nuova; *SEC* South-East Crater

nounced topography originate from the summit conduit: here magma rises, often feeding summit eruptions, and subsequently propagates laterally, downslope, feeding radial fissures (i.e., Rubin and Pollard 1987; Fig. 1). This mechanism has been commonly observed in Hawaii, at both Kilauea and Mauna Loa volcanoes (Decker 1987; Dvorak and Nakamura 1987; Fiske and Jackson 1972; Holcomb 1987; Lockwood et al. 1987). Other examples of summit eruptions being followed by flank eruptions include Mount Etna (Bousquet and Lanzafame 2001; McClelland et al. 1989), Vesuvio (Alfano and Friedlaender 1929 and references therein), Nyiragongo (Tedesco 2002), Miyakejima (Geshi et al. 2002), Izu-Oshima (Sumner 1998), Taveuni (Cronin et al. 2001), Huaynaputina (Adams et al. 2001) and Piton de la Fournaise (McClelland et al. 1989).

A few flank eruptions, however, are triggered by intrusions that are not fed through the summit conduit, as shown by the lack of seismicity, surface deformations and volcanic activity in the latter: examples include Miyakejima (McClelland et al. 1989), Fernandina (Jonsson et al. 1999) and Etna (Romano 1982). These eruptions are possibly directly fed, through radial dikes, by the reservoir beneath the volcano, as proposed at Fernandina (Chadwick and Dieterich 1995). Flank eruptions that are not fed by the summit are here termed peripheral eruptions (Fig. 1).

A stress field controlled by regional tectonics has been commonly invoked to explain the dynamics of lateral flow of magma from a reservoir and thus the occurrence of peripheral eruptions (Gudmundsson 1987, 1998). Nevertheless, all the mentioned peripheral eruptions occurred within volcanic edifices at least 2,000 m high: this suggests that, as an alternative to a regional component, peripheral volcanic activity may also be, even though to a lesser extent (Gudmundsson 2002), influenced by a component due to the load of the volcano.

Peripheral eruptions thus appear to be extremely rare and associated with regional stress fields or prominent (height >2,000 m) volcanic edifices. In order to get more

insights into the dynamics of flank eruptions, trying to better evaluate the role of tectonics and topography, we review the eruptive history of Etna volcano over the last 100 years, for which a database is presented. In particular, we consider the Etna eruption of July–August 2001, which actually was both a summit eruption and a "peripheral" eruption (Lanzafame et al. 2003; Behncke and Neri 2003). The collected data suggest that the regional tectonic stress field played a major role in triggering the peripheral eruption, while the gravitational stresses resulting from the load of the volcano controlled the summit eruption.

Etna and its summit and flank eruptions over the last 100 years

Etna is located at the front of the Apennine-Maghrebian Chain (Cristofolini et al. 1979; Lanzafame et al. 1997a), along the N-S trending extensional Malta escarpment (inset in Fig. 2) and lies on Pliocene-Pleistocene foredeep deposits (mainly sand and clay). Its tectonic setting is characterized by an overall E-W extension direction (Bousquet and Lanzafame 1986; Di Geronimo et al. 1978; Kieffer 1985; Labaume et al. 1990; Lanzafame et al. 1997a, 1997b; Monaco et al. 1997; Monaco and Tortorici 2000).

Volcanism at Etna evolved from a predominantly subaerial and submarine activity along a fissure (up to 200 ka) to the development of several vents dispersed over a wide area (Calvari et al. 1994; Coltelli et al. 1994; Corsaro et al. 2002; Romano 1982). The present Etna has a central conduit, with four summit craters, immediately west of the Valle del Bove depression (Fig. 2). Volcanic activity is focused at the summit and along radial fissures, forming three main "rift zones" (Rittmann 1973; Garduño et al. 1997, and references therein): the NE Rift, the S Rift and the W Rift (Fig. 2). The propagation of the rift zones from the summit craters suggests that the former are laterally fed by the central conduit rather than vertically, directly from the magma reservoir (Bousquet and Lanzafame 2001; Ferrari et al. 1991; Garduno et al. 1997; Kieffer 1985; McGuire and Pullen 1989; Tanguy and Kieffer 1993; Tazieff and Le Guern 1971).

We summarize the modalities of the summit and flank eruptions at Etna over the last 100 years, for which a database is presented; the overview of the eruptive fissures is shown in Fig. 3 and the main features of the eruptions are listed in Table 1.

Many eruptive fissures above 2,000 m have an overall N-S orientation, whereas several fissures below 2,000 m (1911, 1923, 1928, 1947, 1971, 1981 and 1989 eruptions) have more scattered trends, mainly propagating towards NE and SE; these trends are parallel to the Valle del Bove upper rim, which has scarps up to 1 km high (Fig. 3). Moreover, the fissures propagating towards NE are associated with fractures with left lateral components of motion (Garduno et al. 1997; Neri et al. 1991), whereas those propagating towards SE are associated with fractures with right-lateral motions (Coltelli et al. 1994). This kinematics is consistent with that of the Pernicana (to the NE) and Ragalna (to the SE) faults, bordering the mobile eastern and southern sectors of the volcano (Fig. 2; Borgia et al. 1992, 2000; Froger et al. 2001; Lo Giudice and Rasà 1992; Merle and Borgia 1996; Neri et al. 1991; Rust and Neri 1996).

The eruptions in the last 100 years show common features. Strombolian activity from the summit craters, lasting several months, precedes the flank eruptions: these occur through fractures associated with the lateral propagation of radial dikes from the summit, whereby the activity ceases. Thus, the radial dikes transfer magma from the summit craters to the lower portions of the volcano along subhorizontal flow paths (Bousquet and Lanzafame 2001; Ferrari et al. 1991; Garduño et al. 1997; Murray 1994; Murray and Pullen 1984; Neri et al. 1991). In the past 100 years, only two flank eruptions (one in 1974 and – in part – one in 2001; Table 1) were not fed by the central conduit, resulting in peripheral activity (Lanzafame et al. 2003; Bottari et al. 1975); the independence of these eruptions from the central conduit was mainly suggested by the lack of volcanic and seismic activity and surface deformations within the central conduit. Summit eruptions in the last century were usually longer (several months), with moderate extrusion rates (<2 m^3s^{-1}); flank eruptions have higher extrusion rates (>10 m^3s^{-1}) and usually have a shorter duration (commonly a few tens of days; inset b in Fig. 3). The scenario of lateral migration of magma from the summit craters can be applied not only to the last century, but also to a significant part of that of the last 34 ka (Gillot et al. 1994; Kieffer 1985; McGuire 1982).

The tectonic fissures consist of tension fractures and normal faults, with vertical displacements of <2–3 m; the cumulative amount of extension, measured directly on the field, is usually <6 m. The faults are usually arranged in grabens, with a width between 10 and 1,400 m.

At Etna, the development of fractures associated with volcanic activity has been interpreted as being due to the emplacement of a dike at depth (Bousquet and Lanzafame 2001 and references therein). However, fracturing as a consequence of dike emplacement is not a general rule (Bonafede and Danesi 1997) and the deformation pattern may be complicated by the presence of a layering with different mechanical properties (Gudmundsson and Brenner 2001; Gudmundsson et al. 2002 and references therein).

The formation of tension fractures or normal faults at the surface usually depends upon the depth of the dike (Bousquet and Lanzafame 2001: a shallow dike, under lower lithostatic pressures, may induce tension fractures; conversely, a deeper dike, at higher confinement pressures, may form shear fractures (Pollard et al. 1983) and thus grabens at the surface. The velocity of propagation of the fractures can be up to a few m/s, similar to the ones inferred for Iceland (Gudmundsson 1995), with mean values between 0.26 ms^{-1} and 0.01 ms^{-1}; the time required

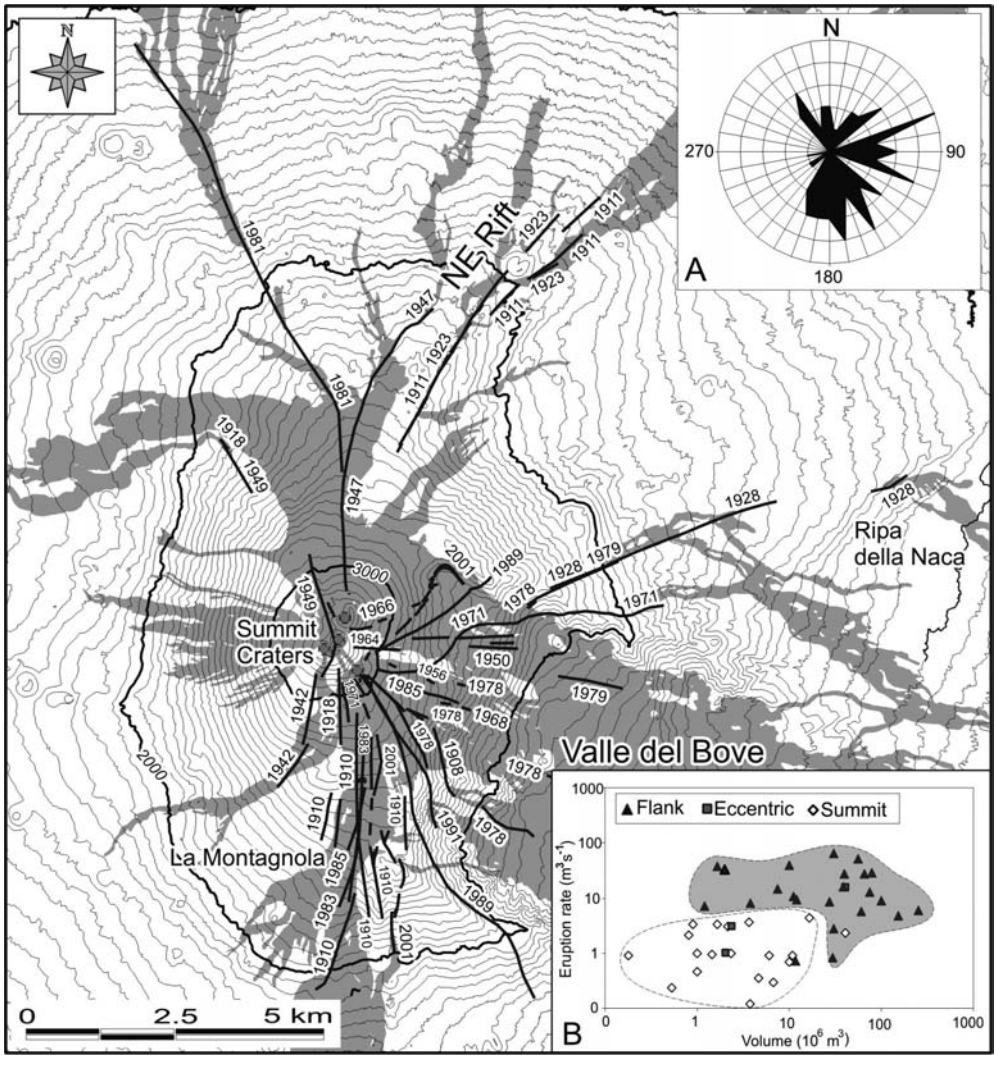

Fig. 3 Location of the eruptive fissures developed at Etna in the last century. *Inset* **A** Rose diagram summarizing the orientation of the eruptive fissures in the last 100 ka. *Inset* **B** Volumes vs. eruption rates of Etnean eruptions in the last century; the domains related to summit and flank eruptions are schematically highlighted (modified from Andronico et al. 2002)

to develop a steady deformation pattern is on the order of a few hundred hours (Table 1).

The 2001 eruption

The Southeast Crater (SEC, Fig. 2inset), one of the four summit craters of Etna, was active, mainly with Strombolian activity, for several years preceding the 2001 eruption, suggesting open central conduit conditions.

A seismic swarm on the southern flank of Etna (Montagnola area, Fig. 4) marked the onset (12–13 July) of the 2001 eruption. Hypocenters of nearly 3,000 earthquakes, aligned along a N-S direction, were mainly located at depths between 3,000 m below and 1,000 m above sea level; nevertheless, a more limited seismicity has been observed down to 4–6 km b.s.l.; no seismicity was recorded below the summit of the volcano (Patanè et al. 2002). Ground swelling (up to 0.2 m) occurred at the Montagnola area on 13 July and continued until the 16th (Bonaccorso et al. 2002). On 16–17 July, a 1,400-m-long, 500-m-wide, NNE–SSW-trending graben formed nearby the parallel Valle del Bove upper rim (area of vent 5 in Fig. 4); total extension across the normal faults was ~3 m, maximum vertical displacement was ~1 m. At this stage, volcanic activity was not observed yet.

During the night of 16–17 July, lava fountaining occurred at the SEC, accompanied by a lava flow (vent 1 in Fig. 4). This was immediately followed by the opening of a N–S-trending eruptive fissure (vent 2 in Fig. 4) at the S base of the SEC. The fissure consisted of tension fractures and normal faults, with a vertical displacement of <0.5 m, forming a ~50-m-wide graben (between vents 2 and 3 in Fig. 4), with a total extension of ~3 m (Fig. 5); the total extension was given by the sum of the openings of the fractures and the openings related to the displacement of the normal faults along a section perpendicular to the fissure. Lava extrusion along this fissure mainly occurred from two vents (vents 2 and 3 in Fig. 4) at 2,950 and 2,700 m, respectively, lasting 23 days. At the onset of effusive activity at vent 3, the effusion rate at vent 2 dropped significantly, suggesting a connection between the vents.

Table 1 Main features of Etna's eruptions in the last century (modified after Andronico et al. 2002). *PR* Piccolo Rifugio, *SC* Serra delle Concazze, *VB* Valle del Bove, *VL* Valle del Bove, *F* flank, *P* peripheral, *S* summit

Onset	End	Duration (days)	Vent location	Type of eruption	Max.-min. vent altitude (m a.s.l.)	Vent length (m)	Fractures				Lava flows			Cumulate lava volume (10^6 m^2)	Pyrocl. volume (10^6m^2)	Mean eruption rate (m^{3}s^{-1})
							Azimuth (°)	Time of propagation (h)	Mean speed of propagation (m/s)	Max. width of the fractures field (m)	Max. length (km)	Area covered (10^6m^2)	Lava volume (10^6m^2)			
29/04/1908	30/04/1908	0.75	Eastern flank: Valle del Bove	F	2,800–2,275	4,250	135;170				4.45	1	2.00	2.00	0.15	33.00
23/03/1910	18/04/1910	27	Southern flank	F	2,300–1,900	5,190	180;210; 225;265	15	0.10	1,410	11.00	4.92	65.00	67.00	0.2	28.00
27/05/1911	10/07/1911	45	NE crater	S	3,160									67.00		
10/09/1911	22/09/1911	13	NE rift	F	2,550–1,625	4,710	30;45	15	0.09		8.50	5.54	55.40	122.40	1.62	50.80
30/11/1918	01/12/1918	2	Northern flank	F	3,100–2,025	1,780	180;325				1.40	0.27	1.22	123.62		7.00
17/06/1923	18/07/1923	31	NE rift	F	2,500–1,800	4,275	30;40	25.5	0.05		11.50	6.48	78.00	201.62	0.5	29.00
02/11/1928	20/11/1928	18	Eastern flank	F	2,700–1,200	4,885	70	56	0.04		9.15	5	40.00	241.62	2.5	27.30
30/06/1942	01/07/1942	0.54	South-western flank	F	2,800–2,500	2,100	185;235	5	0.12	60	4.10	0.83	1.66	243.28	0.1	37.60
24/02/1947	10/03/1947	15	Northern flank	F	3,050–2,200	5,200	355;0;20; 40	18	0.08	150	6.60	1.98	11.88	255.16	0.025	9.20
02/12/1949	05/12/1949	3	Summit area; north-western flank	S–F	3,240–1,990	3,095	210;340; 330	13	0.07		4.60	2.87	10.00	265.16	0.2	39.30
25/11/1950	01/12/1951	372	Eastern flank: Valle del Bove	F	2,850–2,200	1,850	90	2	0.26	400	9.70	10.88	151.36	416.52	0.632	4.73
18/07/1955	02/12/1955	136	NE crater	S	3,200						2.4	1.45	3.63	420.15	0.6	3.60
28/02/1956	02/03/1956	4	Central crater; eastern flank: VB	S–F	3,300–2,700	155	130				2.6	0.31	0.90	421.05	0.21	3.30
02/04/1956	08/04/1956	6	Central crater	S	3,300						4.5	0.55	1.64	422.69	0.567	3.36
16/04/1957	03/05/1957	18	NE crater	S	3,200						1.3	0.48	1.44	424.13		0.93

Table 1 (continued)

Onset	End	Duration (days)	Vent location	Type of eruption	Max.-min. vent altitude (m a.s.l.)	Vent length (m)	Fractures				Lava flows			Cumulate lava volume (10^6 m^2)	Pyrocl. volume (10^6m^2)	Mean eruption rate (m^{3}s^{-1})
							Azimuth (°)	Time of propagation (h)	Mean speed of propagation (m/s)	Max. width of the fractures field (m)	Max. length (km)	Area covered (10^6m^2)	Lava volume (10^6m^2)			
01/02/1964	30/06/1964	150	Central crater; eastern flank: VB	S	3,300–2,900	795	95				3.8	1.84	4.60	428.73		0.35
13/01/1966	31/12/1966	353	NE crater	S–F	3,250–3,070	415	90				2.5	2	3.80	432.52		0.12
07/01/1968	14/07/1968	190	Eastern flank: Valle del Bove	S–F	3,050–2,600		130;70				2.4	0.581	1.45	433.97		0.09
05/04/1971	12/06/1971	69	SE crater; eastern flank: VB, SC	S–F	3,050–1,800	5,172	65;80; 145;170	110	0.01		7.25	7.6	75.00	508.97	3	13.00
30/01/1974	17/02/1974	17	Western flank	P	1,670						1.5	0.3	2.40	511.37	2.025	3.00
11/03/1974	29/03/1974	18	Western flank	P	1,650						1.3	0.2	2.10	513.47	1.075	1.00
10/10/1974	25/02/1975	138	NE crater	S	3,200							1.81	10.90	524.37		0.91
24/02/1975	29/08/1975	187	NE rift	F	2,625						1.75	2.1	11.76	536.13		0.73
12/09/1975	28/11/1975	77	NE crater	S	3,200						2.2	1	6.00	542.13		0.91
29/11/1975	08/01/1977	406	Northern flank: Punta Lucia	F	2,980–2,900						8.00	4.9	29.40	571.53		0.84
16/07/1977	27/03/1978	254	NE crater	S	3,200						7	3.33	6.66	578.19	0.005	0.30
29/04/1978	05/06/1978	37	SE crater; eastern flank: VB	F	3,000–2,600	1,865	140;150	20	0.03		4.00	2.3	27.50	605.69		8.60
25/08/1978	30/08/1978	5	SE crater; eastern flank: VB	S–F	3,050–2,350	1,865	50				2.70	1	4.00	609.69		7.70
23/11/1978	30/11/1978	8	SE crater; eastern flank: VB	F	3,050–1,675		110;160				4.70	3.4	11.00	620.69		10.60

Table 1 (continued)

Onset	End	Duration (days)	Vent location	Type of eruption	Max.-min. vent altitude (m a.s.l.)	Vent length (m)	Fractures				Lava flows			Cumulate lava volume (10^6 m^2)	Pyrocl. volume (10^6m^2)	Mean eruption rate (m^{3}s^{-1})
							Azimuth (°)	Time of propagation (h)	Mean speed of propagation (m/s)	Max. width of the fractures field (m)	Max. length (km)	Area covered (10^6m^2)	Lava volume (10^6m^2)			
03/08/1979	09/08/1979	6	SE crater; eastern flank: VB, SC	F	2,950–1,700	3,825	130;100; 65				6.00	2.5	7.50	628.19		14.50
01/09/1980	26/09/1980	25	NE crater	S	3,200						4	0.33	0.99	629.18		0.46
05/02/1981	07/02/1981	2	NE crater	S	3,200						2	0.03	0.18	629.36		0.91
17/03/1981	23/03/1981	6	North-western flank	F	2,550–1,140	8,045	355;330; 320	33	0.07		7.50	7.4	30.00	659.36	3.3	64.00
28/03/1983	06/08/1983	131	Southern flank: Piccolo Rifugio	F	2,680–2,250	2,580	185;200	12	0.06		7.50	6	100.00	759.36	0.015	8.80
28/04/1984	17/10/1984	172	SE crater; eastern flank: VB	S	3,050						3	1.3	10.00	769.36	0.22	0.70
10/03/1985	13/07/1985	125	SE crater, southern flank: PR	F	3,050–2480	1,095	190;195	6	0.05		3.80	2.7	30.00	799.36	0.025	2.80
25/12/1985	31/12/1985	5	Eastern flank: Valle del Bove	S	2,750–2,420	940	105;110				3.50	0.9	0.80	800.16	0.085	2.10
13/09/1986	24/09/1986	11	NE crater	S	3,240						1.3	0.16	1.00	801.16	3	1.00
30/10/1986	01/03/1987	122	Eastern flank: VB, SE crater	F	3,050–2,180	2,575	75;90	12	0.06		5.00	6.5	60.00	861.16		5.70
11/09/1989	09/10/1989	29	SE crater, eastern flank: VB	F	3,050–2,550	8,740	65;155	192	0.01		8.00	6.4	38.40	899.56		15.90
04/01/1990	02/02/1990	29	SE crater	S	3,050						3	0.73	2.15	901.71	20	3.10
14/12/1991	31/03/1993	473	Eastern flank: Valle del Bove	F	3,100–2,400	2,865	150;165	22	0.04		8.75	7.6	250.00	1,151.71		6.10
04/07/1996	30/07/1996	26	NE crater	S	3,200						1.3	0.18	0.53	1,152.24		0.23
19/07/1997	07/07/1998	353	SE crater	S	3,100						0.8	0.4	2.36	1,154.60		1.01

Table 1 (continued)

Onset	End	Duration (days)	Vent location	Type of eruption	Max.-min. vent altitude (m a.s.l.)	Vent length (m)	Fractures				Lava flows			Cumulate lava volume (10^6 m^2)	Pyrocl. volume (10^6m^2)	Mean eruption rate (m^3s^{-1})
							Azimuth (°)	Time of propagation (h)	Mean speed of propagation (m/s)	Max. width of the fractures field (m)	Max. length (km)	Area covered (10^6m^2)	Lava volume (10^6m^2)			
04/02/1999	14/11/1999	282	SE crater	S–F	3,200–2,920		150;110				2.8	1.35	30.00	1,184.60		1.94
17/10/1999	05/11/1999	19	Bocce Nuova	S	3,300						4	3	16.70	1,201.30		4.30
17/07/2001	09/08/2001	23	SE crater, southern flank, VL	S–F–P	3,000–2,100	7,000	165;195; 180;45	79	0.02	500	6.9	5.57	25.29	1226.59	5–10	12.15

At 00:20 GMT on 18 July, a fracture system opened at 2,100 m to the south of the Montagnola, feeding a lava flow (vent 4 in Fig. 3). A set of N–S vents progressively formed upslope, connecting with the previously formed fault bordering the eastern Montagnola graben.

A further vent (5 in Fig. 4) formed at 17:00 GMT on 19 July, within the southern part of the graben, at Piano del Lago (2,570 m), just north of the Montagnola. The activity here began with the collapse of pit craters, which became the site of intense phreatomagmatic activity (Behncke and Neri 2003) and, 5 days later, of Strombolian and effusive activity. There is evidence of an interdependence between the 2,100-m (vent 4) and the 2,570-m (vent 5) vents: the shift to Strombolian and effusive activity at vent 5 corresponded to a drastic decrease in the effusion rate at vent 4, with a reversal to a higher effusion rate coinciding with the return to phreatomagmatic activity at vent 5 after 1 August. Vents 4 and 5 were active for 23 days, extruding approximately 75% of the total volume of the erupted products and feeding the longest single lava flow of the eruption.

On 20 July, a 1,800-m-long fissure developed at the northern base of the SEC cone, propagating downslope towards NE to 2,680 m (vent 6 in Fig. 4); here Strombolian activity fed a lava flow for 10 days. The fissure consisted of en-echelon tension fracture segments, without vertical displacement and a total extension of 2 m for each segment.

The magmas erupted from vents 4 and 5 (Montagnola area) are less evolved than the rest of the erupted magmas. They contain amphibole xenocrysts and xenoliths from the sedimentary basement, suggesting rapid magma uprise; petrochemical data suggest that these magmas evolved within a closed system (Research Staff of the INGV 2001). The magmas erupted from the radial dikes propagating from the summit show a high porphyritic index; these magmas experienced higher degrees of differentiation, refilling and degassing in a nearly open system, similar to the one which fed the summit craters during the past few decades (Research Staff of the INGV 2001). Nevertheless, despite the different ascent histories, the petrochemical data of the magmas erupted from vents 4 and 5 and from the radial dikes point to a common parent magma, derived from the same deep source (Research Staff of the INGV 2001).

Interpretation of the 2001 eruption

In summary, the 2001 eruption was characterized by a peripheral graben (Montagnola) and two fissures radiating from the summit. The formation of the Montagnola graben and the onset of the related volcanism was preceded by seismicity and elastic deformation (inflation of Montagnola area). Seismic and geodetic data highlight the ascent of magma beneath the Montagnola, mainly from −3,000 m to +1,000 m, along a N-S trend. The emplacement of a ~N–S dike at shallower levels (16 July) induced anelastic deformation, such as the Montagnola graben (Fig. 6): the

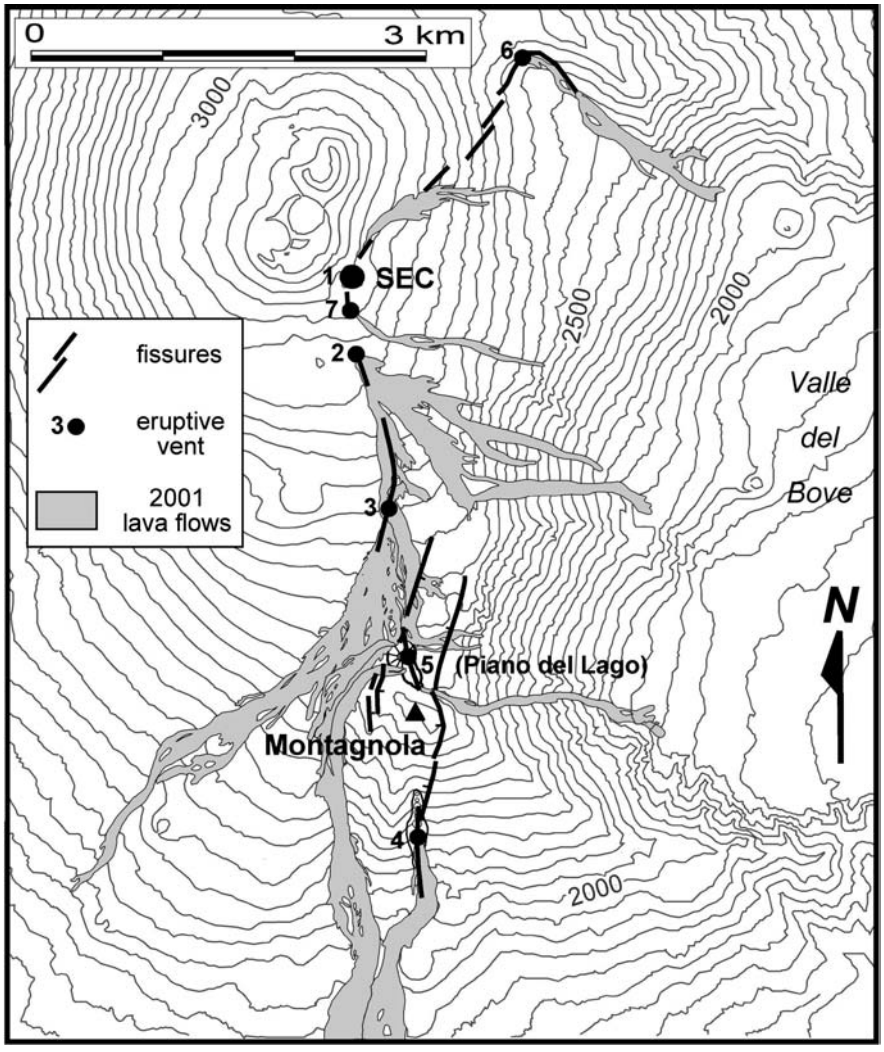

Fig. 4 Overview of the 2001 Etna eruption. The deformation pattern developed during the eruption is highlighted. *Numbers* refer to the chronology of the vents

Fig. 5 View of the N–S-trending radial fissure propagating from the summit crater towards south in the 2001 eruption (vent 3 in Fig. 4 is on the *right*). The fissure is characterized by tension fractures, normal faults and volcanic activity; their width is indicated by the *arrows*

slightly different orientation (~NNE-SSW) of the graben may have been partly controlled by the presence of the nearby parallel Valle del Bove upper rim. Considering a mean dip of 60° for the normal faults bordering the graben, fracturing at surface possibly occurred when the dike was ~500 m below the Piano del Lago (2,570 m a.s.l.), at ~2,100 m. The formation of the vents at 2,100 m is interpreted as being due to the intersection of the dike with topography. The upslope propagation of volcanic activity at vent 4 indicates the subsequent vertical (upward) propagation of the dike. Its central part reached the surface 40 hours later at Piano del Lago. The extension measured at the surface (including the openings of the fractures and those related to the displacement of the normal faults) suggests that the dike, at a depth of a few hundred of meters, was at least 3 m wide.

The N–S (2, 3 and 7 in Fig. 4) and NE–SW (6 in Fig. 4) fissures radiating from the SEC (summit conduit) were characterized by fracturing and volcanic activity progressively migrating downslope. We interpret these as being due to dikes radiating from the summit and transferring magma laterally towards lower elevations. The fact that

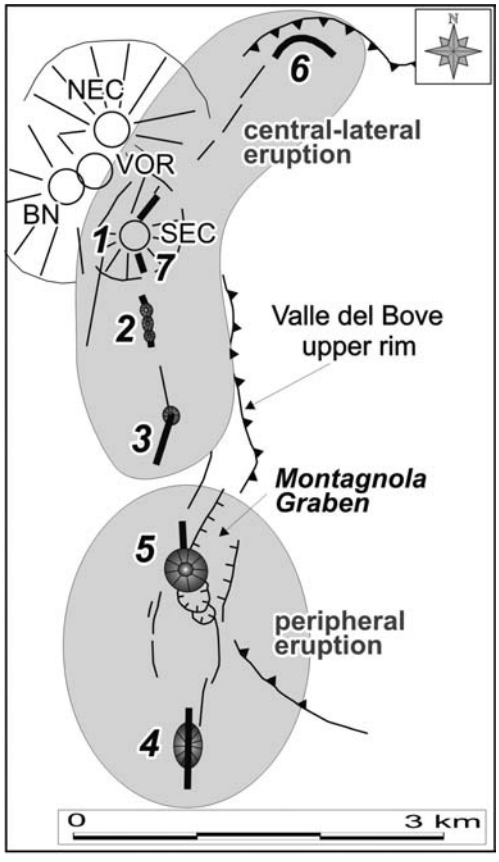

Fig. 6 Interpretation of the eruptive systems developed during the 2001 eruption. The coeval activity of a summit (vents *1*, *2*, *3*, *6* and *7*) and a peripheral (vents *4* and *5*) system is inferred

the fractured area is, in both the radial fissures, approximately a few tens of meters wide, suggests that the propagating tip of the dikes, responsible for fracturing, was shallow (less than a few tens of meters). In these cases, the dikes did not reach the surface, possibly because of the locally higher topography, which was not reached by the upper tip of the propagating dike.

The 2001 Etna eruption was thus characterized by the emplacement of a peripheral vertically propagating, deeper dike (peripheral system) and two radial laterally propagating, shallower dikes, fed by the central conduit system (Fig. 6). The radial dikes and the Montagnola dike showed differences in the surface deformation pattern, depth of emplacement, direction of flow of magma, extrusion rates, eruptive styles and the petrochemical features of the erupted magmas. The intrusion at the Montagnola is thus interpreted as peripheral magmatic system, independent from the magmatic systems of the central conduit system that fed the SEC and the two radial dikes.

A model for the summit-lateral and peripheral 2001 Etna eruption

The lateral propagation of radial dikes transferring magma from the summit to the flanks of the volcano (Bousquet and Lanzafame 2001; Ferrari et al. 1991; Garduño et al. 1997; Murray 1994; Murray and Pullen 1984; Neri et al. 1991) is the classical Etna eruption "type," as shown in Table 1. The emplacement of a peripheral dike distinct from the summit system is a rare event. In the past 100 years, this occurred during the 1974 eruption only (Bottari et al. 1975).

Volcanic activity related to the central conduit system during the 2001 eruption occurred after the emplacement, at very shallow levels, of the peripheral dike. Several features exclude a shallow connection between the summit and the peripheral magmatic systems during the eruption: (1) the lack of seismicity in the area between the Montagnola and the summit; (2) the lack of structural evidence of a northward (towards the summit craters) propagation of the peripheral dike; (3) the lack of any correlation between the increase or decrease of the volumes of erupted magma in the two magmatic systems.

Thus, two main mechanisms can be theoretically invoked for the summit-lateral activity accompanying the peripheral eruption:

1. A variation of the stress field in the area of the summit conduit (central conduit system) due to the emplacement of the peripheral dike. In this case the emplacement of the peripheral dike may have induced stress perturbations at its along-strike tips (northern and southern portions); this may have thus enhanced fracturing in the previously open summit system, filled with residual magma.
2. A connection between the summit and the peripheral magmatic systems at deeper crustal levels (at least below −3 km, which is the bottom depth of the main hypocenter cluster during the seismic swarm). In this case, the magma feeding the peripheral dike is responsible for an increase in the magmatic pressure at the bottom of the column of residual magma within the summit conduit.

The extent of the stress perturbations induced at the tips of the dikes is controlled, among various factors, by the presence of mechanical anisotropies, such as rock layers with different stiffness (Gudmundsson and Brenner 2001; Gudmundsson et al. 2002). However, studies on the stress perturbations resulting from dikes or filled cracks in anisotropic (e.g., Pollard and Aydin 1984; Rubin 1992) and isotropic materials (Thorwarth and Dahm 2002) show that the perturbed area extends along the strike of the dike for no more than 20% of its length. These results are consistent with results from analogue models of dike emplacement in isotropic materials, showing that the maximum extent of the along strike perturbation due to diking is less than 21% of the length of the dike (Acocella et al. 2002). Field and seismic data suggest that the

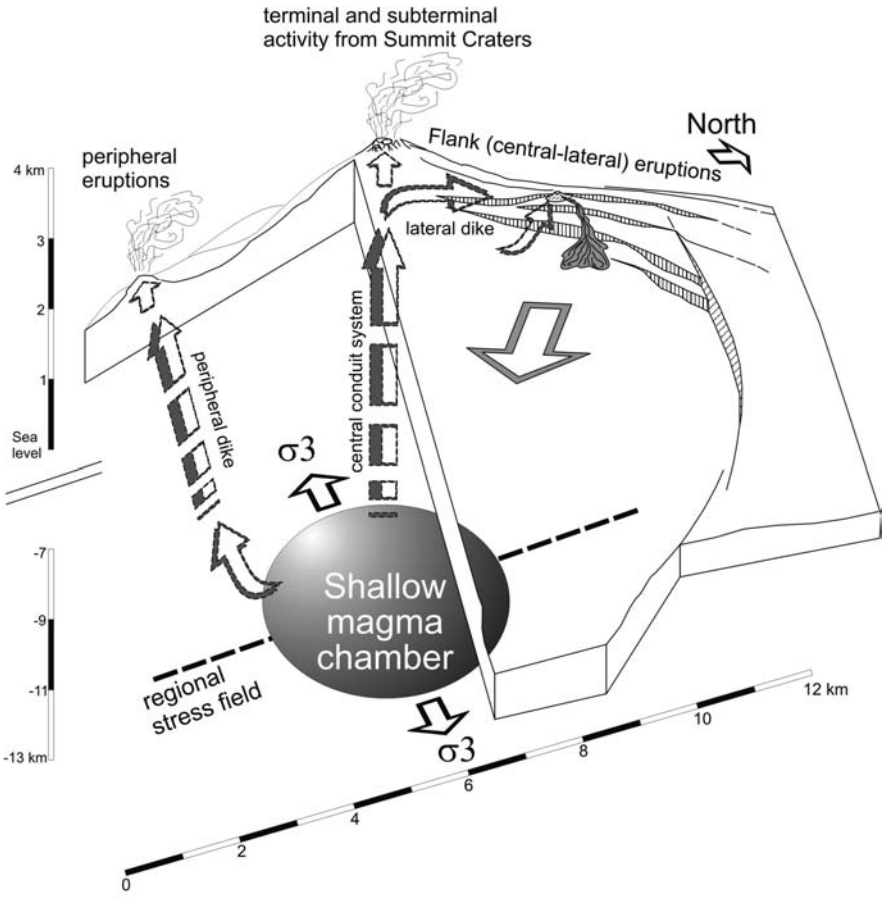

Fig. 7 Proposed model, not to scale, for the control on the 2001 Etna eruption. The rise of the peripheral dike is interpreted to be the result of the regional tectonic stresses acting from depth to shallow levels. Conversely, at the surface, the extrusion of magma is mainly controlled by the gravitational stresses imposed by the load of the volcano. *Vertical scale* is approximate; *horizontal scale* refers to surface

peripheral dike is ~2.5 km long; thus, its emplacement may induced perturbations within ~0.6 km at its tips. The 2-km distance between the northern tip of the dike and the summit does not support the hypothesis that the emplacement of the peripheral dike has modified the stress field within the summit conduit, triggering an eruption. We thus interpret the summit activity at Etna as being due to the same deep input of magma, emplacing a peripheral dike and triggering an eruption of "residual" magma within the summit system. The extrusion of two different types of magma, partly from an open conduit, over a broad distance (more than 4 km) suggests that the 2001 eruption was directly fed by a large reservoir and not by smaller, isolated and shallower magma batches. According to the most up-to-date study, the most likely and significant magma reservoir possibly responsible for the eruption lies at 10 km below sea level (Murru et al. 1999).

The 2001 Etna eruption shows that, even though the summit magmatic system was open, a dike not related to the summit system was emplaced across the flank of the volcano. Three hypotheses may explain the emplacement of the peripheral dike: (1) a peripheral input of magma, which enhances a peripheral extrusion as compared to a central one; (2) the control of gravitational stresses, induced by the eastward sliding of the volcano; (3) a regional tectonic control, which drains magma away from the reservoir at depths between 10 and 3 km b.s.l.

Since the reservoir from which the erupted magma possibly originated lies below the summit craters (Murru et al. 1999), there is no reason to support a peripheral input of magma from the reservoir; thus, the first hypothesis seems unlikely. Deep (~5 km b.s.l.) décollements have been inferred beneath Etna (Borgia et al. 1992); however, these are far much shallower than the possible source of the extruded magma, at 10 km b.s.l.: thus, the ascent of a ~N-S-trending peripheral batch of magma between 10 and at least 5 km b.s.l. occurred at deeper levels and independently from the activity of deep gravitational stresses. These considerations thus suggest a predominant tectonic control of N–S trending structures on the rise of the magma responsible for the 2001 Etna eruption. These N–S-trending structures may be related to the regional systems forming the active N–S-trending Malta escarpment. In this framework, regional tectonics allows the rise of magma from the reservoir from deep levels to shallower levels, permitting the development of N–S-trending peripheral eruptions.

Nevertheless, despite the fact that regional tectonics controlled the ascent of magma, the modalities of fracturing and extrusion at surface were largely controlled by a shallower stress field, related to gravitational stresses as a consequence of the eastward slide of the volcano. This is supported by the trend of the graben and the location of the eruptive fissures fed by the central conduit

system, which follow the paths of previous eruptive fissures; the graben and the fissures are parallel to the Valle del Bove upper rim and follow the trajectories of minimum confinement due to the presence of the Valle del Bove depression (Fig. 3). This fact is confirmed by analogue models of deformations induced by the rise of magma (Acocella et al. 2001); these suggest that the fissures radiating from the summit are the result of the intrusion of magma within the shallowest part of the summit conduit, where a lack of confinement may be present. The intrusions increase the volume of the upper part of the summit, and, where confinement is lacking, they create radial fractures subsequently intruded by magma feeding the radial fissures.

We thus propose a model for the 2001 Etna eruption where different stresses act at different crustal levels (Fig. 7). We suggest that, at depth, the rise of magma responsible for the 2001 Etna eruption was triggered and controlled by N–S-trending regional systems; this permitted the emplacement of a ~N–S-trending peripheral dike during the eruption. Nevertheless, gravitational stresses at surface were responsible for the extrusion of magma along the radial fissures fed by the summit conduit.

Conclusions

The last century of activity at Etna is considered for improving our understanding the dynamics of summit and flank eruptions. Peripheral eruptions (flank eruptions independent from the summit conduit) are very rare at Etna and occurred in 1974 and 2001 only. The 2001 eruption showed both a summit-lateral eruption, feeding two radial dikes, and a peripheral eruption, independent from the summit system. Even though the summit and the peripheral magmatic systems evolved independently at shallow depths (<3 km b.s.l.), the collected data suggests that a common magma from a deep reservoir rose through the two systems. This induced the extrusion of residual magma in the summit system and new magma in the peripheral system. We review the different possible causes triggering the eruption: among these, regional structures are the most likely to have controlled the rise of magma feeding the peripheral eruption. Gravitational stresses predominate, instead, at the surface, controlling the emplacement of the dikes radiating from the summit, parallel to the Valle del Bove upper rim. In this framework, long-term monitoring of the crustal deformations in the Etna area is an essential help to better define the relationships between regional tectonics and flank volcanic activity and thus to better understand the modalities (duration, extrusion rates) of peripheral eruptions.

Acknowledgements The authors wish to thank F. Barberi and R. Funiciello for their encouragement. R. Funiciello provided unique data on the historical flank eruptions of Vesuvio. A. Billi, G. Giordano and G. Lanzafame participated in the field work. B. Behncke provided useful suggestions and improved the English. The reviewers A. Gudmundsson and O. Merle and the editor R. Cioni provided useful comments. This work was partly financed by GNDT funds (under the responsibility of C. Faccenna).

References

Acocella V, Cifelli F, Funiciello R (2001) The control of overburden thickness on resurgent domes: insights from analogue models. J Volcanol Geotherm Res 111:137–153

Acocella V, Cifelli R, Funiciello R, Minore L (2002) Analogue models of dike emplacement. Proceedings EGS meeting Nice, France, April 2002, Abstract vol, p 112

Adams N.K, de Silva S.L, Self S, Salas G, Schubring S, Parmenter JL, Arbesman K (2001) The physical volcanology of the 1600 eruption of Huaynaputina, southern Peru. Bull Volcanol 62:493–518

Alfano GB, Friedlaender I (1929) La storia del Vesuvio. Verlag Dr Karl Höhn, Ulm a.D., p 67

Andronico D, Lodato L, Neri M (2002) Analysis of the 20th century effusive activity at Mount Etna to assess the potential effusive hazard. Proceedings EGS Meeting Nice, France, April 2002

Behncke B, Neri M (2003) The July–August 2001 eruption of Mount Etna (Sicily). Bull Volcanol (in press)

Bonaccorso A, Aloisi M, Mattia M (2002) Dike emplacement forerunning the Etna July 2001 eruption modeled through continuous tilt and GPS data. Geophys Res Lett (in press). DOI 10.1007/s00445-003-0274-1

Bonafede M, Danesi S (1997) Near-field modifications of stress induced by dyke injection at shallow depth. Geophys J Int 130:435–448

Borgia A, Ferrari L, Pasquarè G (1992) Importance of gravitational spreading in the tectonic and volcanic evolution of Mt. Etna. Nature 357:231–235

Borgia A, Lanari R, Sansosti E, Tesauro M, Berardino P, Fornaro G, Neri M, Murray JB (2000) Actively growing anticlines beneath Catania from the distal motion of Mount Etna's decollement measured by SAR interferometry and GPS. Geophys Res Lett 27:3409–3412

Bousquet JC, Lanzafame G (1986) Déformations compressives quaternaires au bord sud de l'Etna. C R Acad Sci Paris 303:235–240

Bousquet JC, Lanzafame G (2001) Nouvelle interprétation des fractures des éruptions latérales de l'Etna: conséquences pour son cadre tectonique. Bull Soc Géol Fr 172:455–467

Bottari A, Lo Giudice E, Patanè G, Romano R, Sturiale C (1975) L'eruzione etnea del gennaio-marzo 1974. Riv Miner Siciliana 154:175–198

Calvari S, Groppelli GL, Pasquarè G (1994) Preliminary geological data on the south-western walls of Valle del Bove, Mt. Etna (Sicily). Acta Vulcanol 5:15–30

Chadwick JR, Dieterich JH (1995) Mechanical modeling of circumferential and radial dike intrusion on Galapagos volcanoes. J Volcanol Geotherm Res 66:37–52

Coltelli M, Garduño VH, Neri M, Pasquarè G, Pompilio M (1994) Geology of the northern wall of Valle del Bove, Etna (Sicily). Acta Vulcanol 5:55–68

Corsaro R, Neri M, Pompilio M (2002) Paleo-environmental and volcano-tectonic evolution of the south-eastern flank of Mt. Etna during the last 225 ka inferred from volcanic succession of the "Timpe", Acireale, Sicily. J Volcanol Geotherm Res 72:1–19

Cristofolini R, Lentini F, Patanè G, Rasà R (1979) Integrazione di dati geologici, geofisici, e metrologici per la stesura di un profilo crostale in corrispondenza dell'Etna. Boll Soc Geol It 98:239–247

Cronin SJ, Bebbington M, Lai CD (2001) A probabilistic assessment of eruption recurrence of Taveuni volcano, Fiji. Bull Volcanol 63:274–288

Decker RW (1987) Dynamics of Hawaiian volcanoes: an overview. US Geological Survey Professional Paper 1350:997–1018
Di Geronimo I, Ghisetti F, Lentini F, Mezzani L (1978) Lineamenti neottettonici della Sicilia orientale. Mem Soc Geol It 19:543–549
Dvorak JJ, Nakamura A (1987) A hydraulic model to explain variations in summit tilt rate at Kilauea and Mauna Loa volcanoes. US Geol Surv Prof Pap 1350:1281–1296
Ferrari L, Garduño VH, Neri M (1991) I dicchi della valle del Bove, Etna: un metodo per stimare le dilatazioni di un apparato vulcanico. Mem Soc Geol It 47:495–508
Fiske RS, Jackson ED (1972) Orientation and growth of Hawaiian volcanic rifts: the effect of regional structure and gravitational stresses. Proc R Soc Lond 329:299–326
Froger JL, Merle O, Briole P (2001) Active spreading and regional extension at Mount Etna imaged by SAR interferometry. Earth Planet Sci Lett 187:245–258
Garduño VH, Neri M, Pasquarè G, Borgia A, Tibaldi A (1997) Geology of the NE Rift of Mount Etna, Sicily (Italy). Acta Vulcanol 9:91–100
Gillot PY, Kieffer G, Romano R (1994) The evolution of Mount Etna in the light of potassium-argon dating. Acta Vulcanol 5:81–87
Geshi N, Shimano T, Chiba T, Nakada S, (2002) Caldera collapse during the 2000 eruption of Miyakejima volcano, Japan. Bull Volcanol 64:55–68
Gudmundsson A (1987) Lateral magma flow, caldera collapse and a mechanism of large eruptions in Iceland. J Volcanol Geotherm Res 34:65–78
Gudmundsson A (1995) The geometry and growth of dykes. In: Baer G, Heimann A (eds), Physics and chemistry of dykes 23–33. Balkema, Rotterdam
Gudmundsson A (1998) Magma chambers modeled as cavities explain the formation of rift zone central volcanoes and their eruption and intrusion statistics. J Geophys Res 103:7401–7412
Gudmundsson A (2002) Emplacement and arrest of sheets and dykes in central volcanoes. J Volcanol Geotherm Res 116:279–298
Gudmundsson A, Brenner SL (2001) How hydrofractures become arrested. Terra Nova 13:456–462
Gudmundsson A, Fjeldskaar I, Brenner SL (2002) Propagation pathways and fluid transport of hydrofractures in jointed and layered rocks in geothermal fields. J Volcanol Geotherm Res 116:257–278
Holcomb RT (1987) Eruptive history and long-term behaviour of Kilauea volcano. US Geol Surv Prof Pap 1350:261–350
Jonsson S, Zebker H, Cervelli P, Segall P, Garbeil H, Mouginis-Mark P, Rowland S (1999) A shallow-dipping dike fed the 1995 flank eruption at Fernandina volcano, Galapagos, observed by satellite radar interferometry. Geophys Res Lett 26:1077–1080
Kieffer G (1985) Évolution structurale et dynamique d'un grand volcan polygénique: stade d'édification et activité actuelle de l'Etna. PhD Thesis, Univ Clermont-Ferrand II, 497 pp
Labaume P, Bousquet JC, Lanzafame G, (1990) Early deformations at a submarine compressive front: the Quaternary Catania foredeep south Mt. Etna, Sicily. Tectonophysics 177:349–366
Lanzafame G, Leonardi A, Neri M, Rust D (1997a) Late overthrust of the Appenine-Maghrebian Chain at the NE periphery of Mt. Etna, Italy. C R Acad Sci Paris 324:325–332
Lanzafame G, Neri M, Coltelli M, Lodato L, Rust D (1997b) North-South compression in the Mt. Etna region (Sicily): spatial and temporal distribution. Acta Vulcanol 9:121–133
Lanzafame G, Neri M, Acocella V, Billi A, Funiciello R, Giordano G (2003) July–August 2001 Etna eruption: deformative pattern and its significance. Journal of the Geological Society of London (in press)
Lo Giudice E, Rasà R (1992) Very shallow earthquakes and brittle deformation in active volcanic areas. The Etnean region as an example. Tectonophysics 202:257–268
Lockwood JP, Dvorak JJ, English TT, Koyanagi RY, Okamura AT, Summers ML, Tanigawa WR (1987) Mauna Loa 1974–1984. A decade of intrusive and extrusive activity. US Geol Surv Prof Pap 1350:537–570
McClelland L, Simkin T, Summers M, Nielsen E, Stein TC (1989) Global volcanism, 1975–1985. Prentice Hall, Englewood Cliffs, 657 pp
McGuire WJ (1982) Evolution of the Etna volcano: information from the southern wall of the Valle del Bove caldera. J Volcanol Geotherm Res 13:241–271
McGuire WJ, Pullen AD (1989) Location and orientation of eruptive fissures and feeder-dykes at Mount Etna: influence of gravitational and regional stress regimes. J Volcanol Geotherm Res 38:325–244
Merle O, Borgia A (1996) Scaled experiments of volcanic spreading. J Geophys Res 101:13805–13817
Monaco C, Tapponier P, Tortorici L, Gillot PY (1997) Late Quaternary slip rates on the Acireale-Piedimonte normal faults and tectonic origin of Mt. Etna (Sicily). Earth Planet Sci Lett 147:125–139
Monaco C, Tortorici L (2000) Active faulting in the Calabrian arc and eastern Sicily. J Geodyn 29:407–424
Murray JB (1994) Elastic model of the actively intruded dyke feeding the 1991–1993 eruption of Mt. Etna, derived from ground deformation measurements. Acta Vulcanol 4:97–99
Murray JB, Pullen AD (1984) Three dimensional model of feeder conduit of the 1983 eruption of Mount Etna volcano, from ground deformation measurements. Bull Volcanol 47:1145–1163
Murru M, Montuosi C, Wiss M, Privitera E (1999) The locations of magma chambers at Mt. Etna, Italy, mapped by b-values. Geophys Res Lett 26:2553–2556
Neri M, Garduño VH, Pasquarè G, Rasà R (1991) Studio strutturale e modello cinematico della Valle del Bove e del settore nord-orientale etneo. Acta Vulcanol 1:17–24
Patanè D, Chiarabba C, Cocina O, De Gori P, Moretti M, Boschi E (2002) Tomographic images and 3D earthquake locations of the seismic swarm preceding the 2001 Mt. Etna eruption: evidence for a dyke intrusion. Geophys Res Lett 29 NO10, 101029/2001 GLO14391
Pollard DD, Delaney PT, Duffield WA, Endo ET, Okamura AT (1983) Surface deformation in volcanic rift zones. Tectonophysics 94:541–584
Pollard DD, Aydin A (1984) Propagation and linkage of oceanic ridge segments. J Geophys Res 89:10017–10028
Research Staff of the Istituto Nazionale di Geofisica e Vulcanologia — Catania, Italy (2001) Multidisciplinary approach yields insight into Mt. Etna eruption. EOS, Trans AGU 52:653–656
Rittmann, A (1973): Structure and evolution of Mount Etna. Philos Trans R Soc Lond 274 A:5–16
Romano R (1982) Succession of the volcanic activity in the Etnean area. Mem Soc Geol It 23:27–48
Rubin AM, Pollard DD (1987) Origins of blade-like dikes in volcanic rift zones. US Geol Surv Prof Pap 1350:1449–1470
Rubin AM (1992) Dike-induced faulting and graben subsidence in volcanic rift zones. J Geophys Res 97:1839–1858
Rust D, Neri M (1996) The boundaries of large-scale collapse on the flanks of Mount Etna, Sicily. In: McGuire WC, Jones AP, Neuberg J (eds) Volcano instability on Earth and other planets. Geol Soc Lond Spec Publ 110:193–208
Sumner JM (1998) Formation of clastogenic lava flows during fissure eruption and scoria collapse: the 1986 eruption of Izu-Oshima volcano, eastern Japan. Bull Volcanol 60:195–212
Takada A (1997) Cyclic flank-vent and central-vent eruption patterns. Bull Volcanol 58:539–556
Tanguy H, Kieffer G (1993) Les éruptions de l'Etna et leurs mécanismes. Mem Soc Geol Fr 163:239–252
Tazieff H, Le Guern F (1971) Signification tectonique et mécanisme de l'éruption d'avril-mai-juin 1971 de l'Etna. C R Acad Sci Paris 272:3252–3255
Tedesco D (2002) The January 2002 eruption of Mount Nyiragongo, DRC: dynamics andhazard. Proc EGS meeting Nice, France, April 2002 Abstract vol, p 111
Thorwarth M, Dahm T (2002) Three-D stress field around a rising fluid-filled crack. Proc EGS meeting, Nice, France, April 2002. Abstract vol, p 308